The efficiency of quartz addition on electric arc furnace (EAF) carbon steel slag stability

D. Mombelli, C. Mapelli, S. Barella, A. Gruttadauria, G. Le Saoût, E. Garcia-Diaz

The efficiency of quartz addition on electric arc furnace (EAF) carbon steel slag stability

D. Mombelli [a,*], C. Mapelli [a], S. Barella [a], A. Gruttadauria [a], G. Le Saout [b], E. Garcia-Diaz [b]

[a] Politecnico di Milano, Dipartimento di Meccanica, Via La Masa 1, 20156 Milano, Italy
[b] Centre des Matériaux des Mines d'Alès (C2MA) —Ecole des Mines d'Alès (Institut Mines Telecom), Avenue de Clavières 6, 30100 Alès cedex, France

HIGHLIGHTS

- A method to stabilize EAF slag was implemented in an actual steel plant.
- The stabilization treatment lead to the formation of slag with gehlenite matrix.
- The stabilization process efficacy was confirmed by several leaching tests.
- Gehlenite inhibits heavy metals leaching.

ABSTRACT

Electric arc furnace slag (EAF) has the potential to be re-utilized as an alternative to stone material, however, only if it remains chemically stable on contact with water. The presence of hydraulic phases such as larnite ($2CaO\ SiO_2$) could cause dangerous elements to be released into the environment, i.e. Ba, V, Cr. Chemical treatment appears to be the only way to guarantee a completely stable structure, especially for long-term applications. This study presents the efficiency of silica addition during the deslagging period. Microstructural characterization of modified slag was performed by SEM and XRD analysis. Elution tests were performed according to the EN 12457-2 standard, with the addition of silica and without, and the obtained results were compared. These results demonstrate the efficiency of the inertization process: the added silica induces the formation of gehlenite, which, even in caustic environments, does not exhibit hydraulic behaviour.

Keywords:
EAF slag
Leaching behavior
Liquid-on-solid ratio
Stabilization process
Quartz addition

1. Introduction

Today steel slag is considered effectively equivalent to the common stone material employed in civil engineering applications. Its physical and mechanical properties are often higher than those of traditional raw materials [1–6] and, in recent decades, its use has increased exponentially [7]. In particular, electric arc furnace slag (EAF) offers several advantages when compared to other aggregates: it lacks clay and organic ingredients in its composition, has a rough and porous surface and provides good adhesion and good abrasion resistance.

Road construction [6,8–12] and concrete/clinker production [13–16] are common applications in which EAF slag could be mixed with or completely replace traditional raw materials. EAF slag could be used as an aggregate in Hot Mix Asphalt (HMA) pavements, as an aggregate in concrete pavements, as a base or sub-base material, as an embankment material and as a railway ballast [17]. Slag aggregates are not directly exposed to the environment when mixed with other substances, i.e. bituminous binders or cement. For such applications, the standards do not generally require elution tests because the slag does not come in contact with water. On the contrary, leaching behavior characterization is mandatory for slag use in unbound applications, i.e. unpaved roads, armourstone or gabions. In such conditions, slag are subject to continuous cycle of wetting and drying. Several studies [4,10,18–20] have investigated the leaching behavior of slag aggregates and highlight that such aggregates could potentially release dangerous chemical elements (especially Ba, V and Cr), as well as unbound slag, when coming into contact with water.

Other investigations of the leaching behavior of EAF slag [21–25] have tried to identify the major mineralogical phases responsible for the dangerous species release. Electric arc furnace slag has a chemical composition close to that of the cement clinker, mainly

* Corresponding author. Tel.: +39 0 223998660.
E-mail addresses: davide.mombelli@mail.polimi.it, dadeviola@alice.it (D. Mombelli).

constituted by calcium-silicates and calcium-ferrites, which makes steel slag potentially usable as a cementitious material [26]. Experimental tests have identified calcium silicates, especially larnite[1], hartrurite and bredigite, as the principal phases reacting with water and thus responsible for the releasing of elements, i.e. barium [22,23]. Other phases might also contribute to an increase in the amount of elements in the eluate: brownmillerite, calcium aluminate and non-stoichiometric spinels could be associated with Cr release. Barium oxide is a substitutional chemical compound of CaO in calcium silicates whereas chromium (in both trivalent or hexavalent form) could replace iron and aluminum oxide in a brownmillerite-type phase [27] and in calcium aluminates [28]. The hydration process facilitates the migration of species such as Ca, Mg or Ba into water. In a basic environment, chromium oxide could be easily dissolved into a hexavalent form, which is the most reactive and dangerous (it is classified as carcinogenic by the World Health Organization).

Hydration process by a dissolution precipitation requires ample time to be completed: for example, pure larnite reaches 50% of the hydrated ratio in 100 days [29]. Therefore, larnite hydration and dissolution is very difficult to be noted in EAF slag during the 24 h of a standard leaching test (EN 12457-2 standard) because only a small amount of the slag, less than 1%, reacts with water. However, this amount is enough to solubilize a quantity of Ba, Cr and V that exceeds the limits imposed by environmental regulations. Since the polluting elements are generally bound to the silicates, reducing their amount or reducing their solubility are two ways to overcome the problem. This could be achieved by promoting the transformation of the phases in which the aluminum is in the tetra-coordinated form and increasing the polymerization degree of the structure, namely increasing the number of SiO_4 tetrahedra. Specifically, the resistance of a silicate to hydration and the hydrolysis processes increases with the degree of oxygen sharing between SiO_4 polyhedra of the mineral structure [30]. These microstructural transformations should lead to the formation of more stable phases featured by high degree of condensation of structural tetrahedra, i.e. anorthite or gehlenite. Breaking the bonds is difficult due to an insufficient ion force of the mixing medium. In this case, the aluminum atoms are situated in tetrahedral coordination and behaves like silicon atoms [31]. Thus, a thermochemical inertization process was developed to transform EAF slag into an absolutely safe by-product useful for both aggregates and unbound applications. The treatment consists in the addition of pure quartz into the fluid slag during the deslagging operation, allows producing a continuous flow of treated slag having specific chemical composition and properties. The dosing device consists in a sand storage container equipped with automatic vibrating delivery table and with a chute positioned downstream the delivery device, to continuously carry the sand in the mixing zone. The admixed slag is collected in a slag-pot, which helps to keep it stirred, thus homogenizing the microstructure. This process is based on the same principle adopted by Drissen et al. [32] to stabilize Basic Oxygen Furnace (BOF) slag. Being the slag treatment only possible at the liquid state, the novelty of the proposed technique is to chemically modify the slag, exploiting its residual heat without external heating source or remelting operations. In this way, no modification inside the furnace are provided, avoiding to compromise the steel quality, and no additional investment's costs are need to successfully treat the slag.

The quartz addition should have a two-fold effect: it reacts with calcium aluminates to form gehlenite, inhibiting the formation of larnite, and simultaneously prevents its disintegration, thus avoiding the "dusting effect" [33]. Larnite undergoes several phase transformations [34], the most important of which is the inversion from β-Ca_2SiO_4 (monoclinic) to γ-Ca_2SiO_4 (orthorhombic). This transformation is accompanied by a volume increase of around 12% [35]. β to γ transformation causes disintegration of the slag, the so called "dusting effect," making slag handling and storage problematic and the achievement of economic value for the slag virtually impossible. Formation of only 4 wt.% of γ-Ca_2SiO_4 is enough to cause slag disintegration. A relatively small amount of SiO_2 is enough to form a large amount of gehlenite [36]. Gehlenite, together with akermanite, is the main crystalline phase in ground granulated blast furnace slag, which is known to have very low hydraulic activity and a low environmental impact [37–39].

This work presents the benefits of silica treatment on slag release behavior. The efficiency of adding silica was experimentally demonstrated by XRD, SEM and leaching test analyses, with regards to liquid-on-solid ratio effects.

Table 1
XRF chemical composition (weight %) and samples identification.

Sample ID	SiO_2	Al_2O_3	CaO	MgO	FeO	Cr_2O_3	V_2O_5	Ba	Λ
S1	12.36	8.96	26.10	3.21	37.53	2.46	0.08	0.06	0.800
S2	10.36	7.26	28.67	3.98	39.69	1.96	0.10	0.08	0.820
MS1	18.34	9.25	23.26	2.85	35.93	2.25	0.09	0.11	0.759
MS2	22.39	8.20	19.18	2.24	37.29	2.01	0.09	0.07	0.739

2. Experimental procedure

Two batches of carbon steel slag (S1 and S2) were investigated and modified (MS1 and MS2) by the above mentioned inertization process. The added quartz has an average particle size between 1 and 5 mm, with the 90% included in the 1–2 mm range. This size assures the sand to completely melt and dissolve itself in the slag flow. The quartz amount is comprised between 5% and 15% by weight of the slag, with optimal values approximately between 8 and 12 wt.%, depending on the initial chemical composition of the slag to be treated.

Slag chemical compositions were measured by XRF and checked by SEM-EDS and are reported in Table 1 together with the sample identification and optical basicity (Λ) (a basicity index formulated by Duffy and Ingram using spectrographic information coupled with the electronegativity data defined by Pauling [40]).

The analyzed slag are located on the phase ternary diagram shown in Fig. 1.

The comparison between as-received (S1 and S2) and modified slag (MS1 and MS2) was performed from a morphological and microstructural point of view with XRD and SEM analyses.

X-ray diffraction (XRD) data was collected using a Bruker D8 Advance diffractometer in a θ–θ configuration and employing Cu Kα radiation (λ = 1.54 Å) with a fixed divergence slit size 0.5° and a rotating sample stage. The samples of powder were obtained by ring mill grinding (average diameter 15 μm) and were scanned between 10° and 80° with the Vantec detector. The qualitative analysis was performed with EVA software.

Morphological and microstructural characterization was performed by Zeiss EVO50 Scanning Electron Microscopy (SEM) equipped with an Oxford Inca EDS probe. The slag was moulded in an araldite-based resin, grinded and polished. SEM analyses were carried out in backscattered electrons mode (BSE) in order to identify and check the different phases pointed out by XRD. General and local chemical compositions were measured using an EDS probe.

The slag leaching behaviour was investigated by performing the standard leaching test according to EN 12457-2 (24 h in 10 l/kg

[1] Refer to "LIST OF PHASES" for the chemical formula.

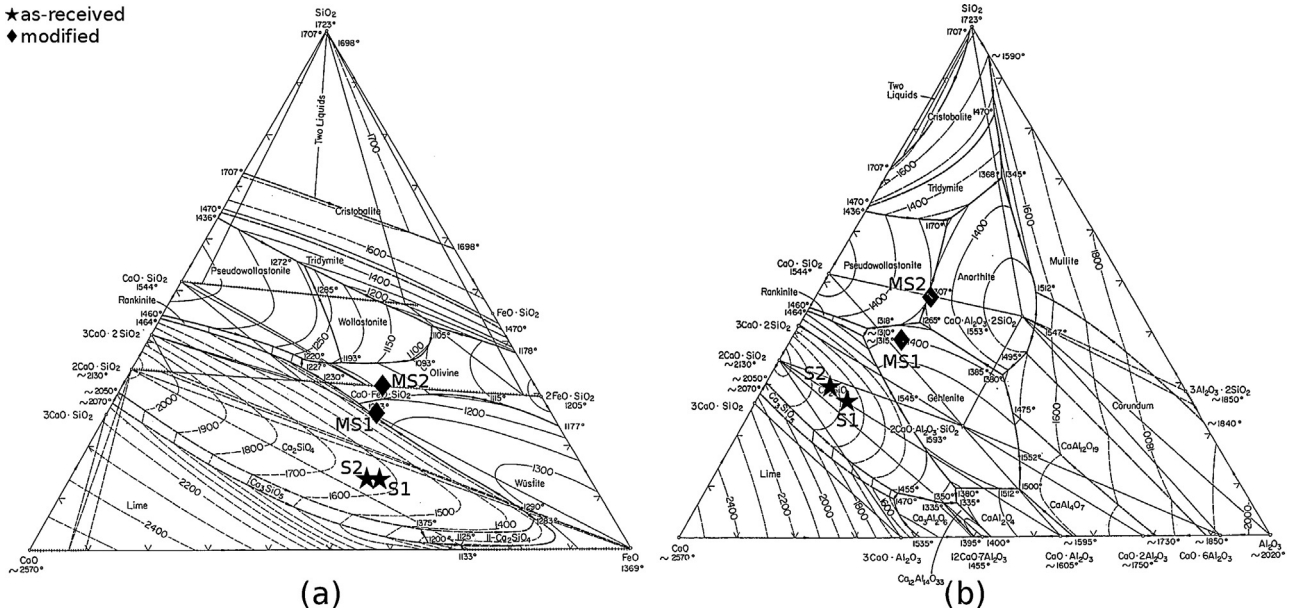

Fig. 1. Samples identification on (a) $CaO–SiO_2–FeO$ and (b) $CaO–Al_2O_3–SiO_2$ phase diagram [42].

deionized water stirred by a rotatory mixer at 10 rpm) on 4 mm of granulated slag. The concentration limits taken as reference are indicated in the Italian legislative decrees ("D.M. 03 August 2005N. 201: definition of the criteria for waste acceptance at landfills" and "D.M. 05 April 2006N. 186: identification of non-hazardous waste subject to simplified recovery procedures"). Because of the slag dissolution rate is dependent on many parameters, i.e. surface-to-volume (S/V) ratio, liquid-to-solid (L/S) ratio, time, temperature and flow conditions [41], beside the standard leaching test, three different experimental conditions were employed:

- Powdered slag leaching behaviour was investigated varying the L/S ratio (10, 100, 1000 l/kg). Weight loss was measured after each test and the dried powders were investigated using XRD.
- Crushed slag particles (average dimension 4 mm) were leached under the same conditions as the standard leaching test and by varying the L/S ratio (10, 100, 1000 l/kg). The slag was characterized by SEM before and after the elution tests conducted in the same areas to detect morphological alterations.
- A polished section of massive grains was leached under the same conditions as the standard test and followed by SEM investigation in order to detect which phases had dissolved. The same test was repeated after 30 days of immersion in deionized water and in two different pH aqueous solutions (pH 10 and pH 4). A pH 10 solution was prepared with 3.5 mg of NaOH in 350 ml of deionized water to simulate the effect of alkaline environment and to verify the possibility to use the slag in concrete production. A pH 4 solution was prepared by adding 3 drops of H_2SO_4 and 3 drops of HNO_3 to 1 l of deionized water to simulate the acid rains.

Water analyses were performed by ICP-OES to determine the chemical species concentration.

3. Results and discussion

3.1. Microstructural characterization

The XRD analysis performed on the slag powder enabled identification of the mineralogical phases featured in the different samples (Fig. 2).

As-received slag was characterized by a large presence of wustite, larnite and a small amount of Mg-Cr-spinels. Traces of gehlenite and brownmillerite were also detected in S1 and S2 samples, respectively (Fig. 3a). SEM analyses confirmed the results of XRD and facilitated the characterization of each structural constituent's morphology and distribution (Fig. 3). As-received samples featured a high percentage of larnite, approximately 37% (S1 sample) and 31% (sample S2), which was estimated by selective dissolution in a methanol-salicylic acid solution [43]. In the S1 sample, Mg-Cr-spinels (Sp in Fig. 3a) and gehlenite islands (G) were finely dispersed in the larnite matrix (L). The wustite (W) had the typical dendritic form. In the S2 sample, the wustite (W in Fig. 3c) appeared thinner and more dispersed than in the S1 slag and was surrounded by brownmillerite-type phases (B). In both batches, chromium was mainly bound in spinel-like phases even if significant amounts were also detected in the brownmillerite, larnite and wustite (Table 2). Vanadium and barium were mainly present in the larnite, brownmillerite and gehlenite in the S1 sample. The presence of such dangerous elements in the hydraulic phases classified the as-received slag as potential dangerous waste.

The thermochemical treatment modified the slag microstructure. As pointed out in the XRD pattern (Fig. 2b), the admixed silica lead to another phase assemblage. In particular, the larnite and brownmillerite reacted with SiO_2 to form gehlenite. In fact, diffraction patterns displayed very intense peaks, typical of gehlenite-akermanite phases, whereas no more reflection of larnite and brownmillerite was detected. In the MS2 sample, secondary peaks were also detected, probably associated with kirschsteinite.

Morphologically, the microstructures appeared homogeneous and were constituted by a gehlenite matrix (G in Fig. 3b–d) in which wustite (W in Fig. 3b–d) and Mg-Cr-spinels (Sp) were dispersed. The stirring effect of the slag-pot probably contributed towards homogenizing the microstructure and completing the diffusive reactions between the different phases. The wustite appeared finer and thinner with pronounced dendritic structures. This aspect was associated with the reduction of the slag melting temperature, which was induced by the quartz addition. Specifically, the admixed quartz significantly reduced the slag's melting temperature, allowing it to maintain the slag mass in a liquid state in the slag-pot for a prolonged period of time. In this way, wustitic dendrites were able

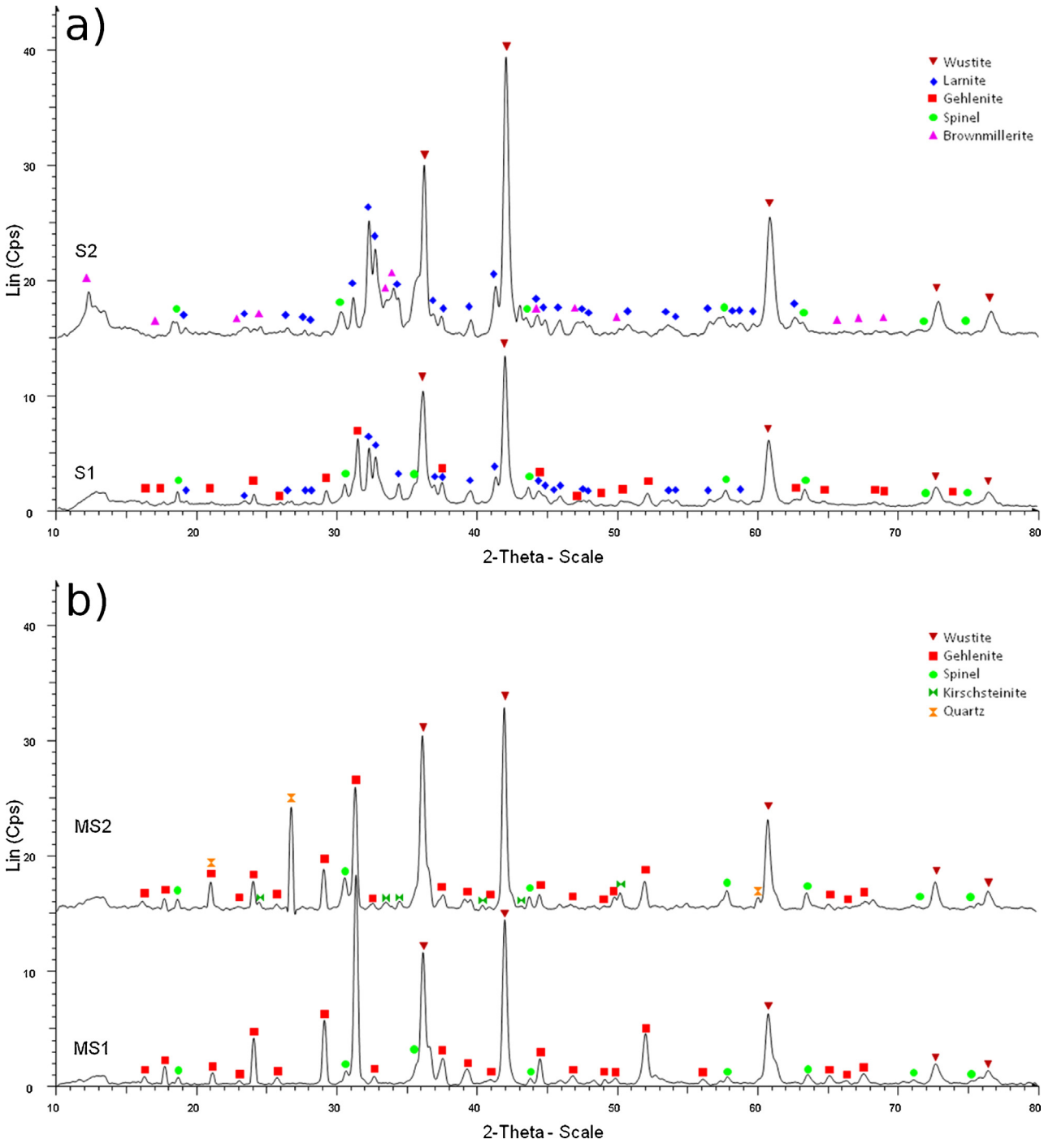

Fig. 2. XRD patterns of (a) as-received and (b) modified slag.

to grow upwards, being surrounded by a totally molten phase. On the contrary, in as-received samples, the wustite solidified within the free spaces between the larnite blocks, which were already solid during the deslagging step.

In the modified slag, the spinels were now aggregated in larger structures. Chromium was completely fixed in these oxides whereas barium had totally migrated into the gehlenite matrix. In this form, the slag should have been completely stable and the release of Ba, V and Cr hindered. Indeed, as reported in several studies on cement and concrete chemistry, gehlenite has poor hydraulic properties, and some researchers consider it as a non-hydraulic phase [29,44].

4. Standard leaching tests

Standard elution tests (Table 3) performed on 4 mm of granulated slag, confirmed the predicted slag behavior from the microstructural analyses. Attention was focused on only the most problematic environmental factors (Ba, V, Cr, pH) as the other substances (requested by the EN 12457-2 standard) were in compliance with the regulation limits. The as-received slag presented barium and vanadium release but no Cr release was detected. In this case, the spinel-like phases were most likely stable and had limited the chromium leaching. Moreover, after the test the water pH had reached values of more than 11.5, close to the upper limit. Under

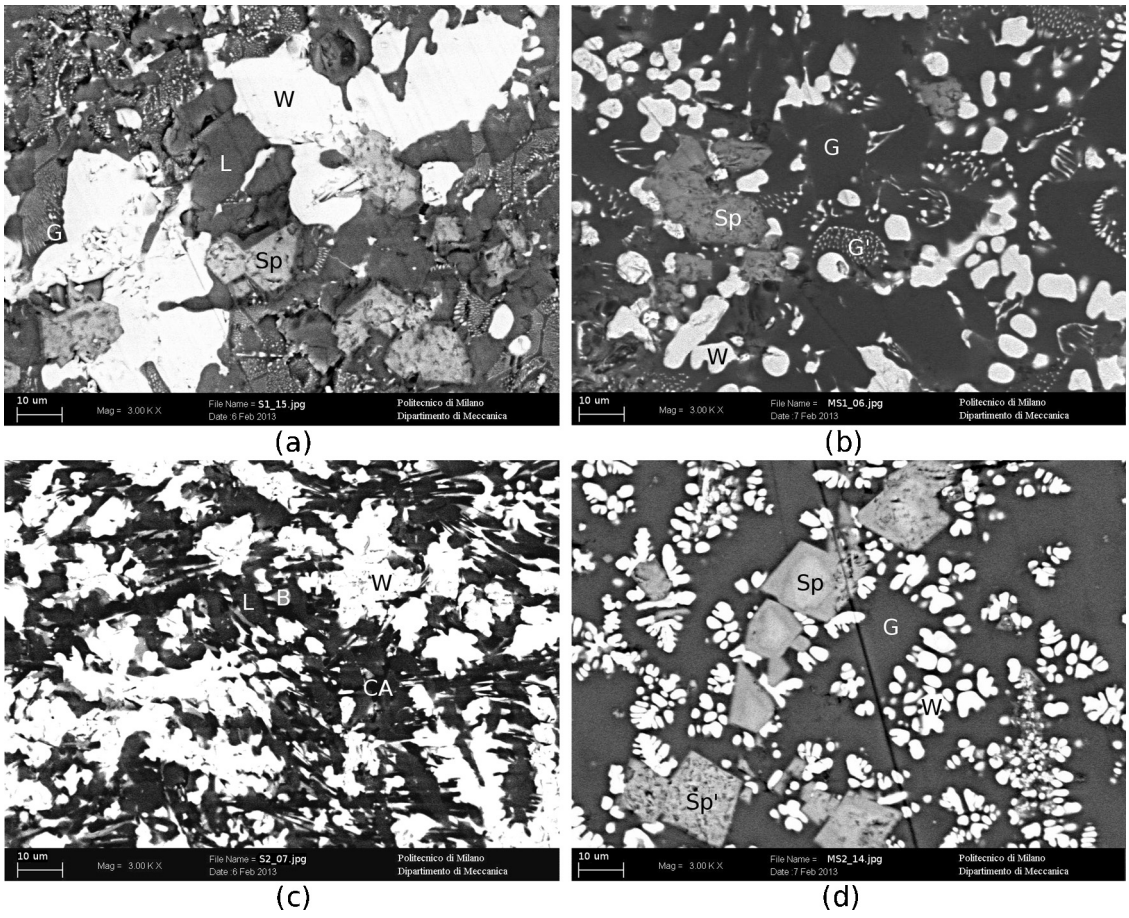

Fig. 3. SEM-BSE micrographies of as-received and modified slag: (a) S1, (b) MS1, (c) S2 and (d) MS2 (B = brownmillerite; CA = calcium aluminate; G = gehlenite; L = larnite; Sp = Mg-Cr-spinel; W = wustite).

these conditions, the environment would be considered caustic, potentially causing severe damage to vegetables, rocks and animals. In this situation, use of the slag without appropriate treatment would be hazardous, including for such applications where the slag is bound.

After the quartz treatment, the pH had decreased significantly and the Ba and V concentrations in the water were below the limit. The results obtained after the standard tests provided evidence of the inertization technique's efficiency. However, to better understand which phases were responsible for elements leaching and to

Table 2
Local chemical composition of phases pointed out by SEM-BSE analysis.

SEM-EDS Analysis (atomic%)												
Sample	Phase	Mg	Al	Si	Ca	Ti	V	Cr	Mn	Fe	Sb	Ba
S1	W	14.66	0.78		2.12		0.03	1.51	9.43	71.36		0.10
	L			33.38	64.31		0.11	0.17		0.88	1.11	0.04
	Sp	16.78	18.30		1.28		0.09	42.80	4.18	16.50		0.07
	G	2.58	31.98	17.15	29.85			0.34	2.29	15.65		0.15
S2	W	15.99	0.84		3.69		0.05	3.20	7.01	69.22		
	L		4.00	30.43	62.60	0.30	0.05	0.15		1.68	0.76	0.03
	B		20.57	4.66	49.08	4.14	0.34	0.59	0.52	19.86		0.25
	CA		38.44	7.09	49.59		0.01	0.03	0.32	3.89	0.54	0.10
MS1	W	5.77	0.89		1.19	0.40	0.10	0.53	8.52	82.59		
	Sp	9.52	24.03		0.83		0.08	36.92	3.82	24.76		0.04
	G	2.71	24.28	28.35	39.38		0.07	0.03	0.51	3.67	0.90	0.11
	G′	2.58	21.07	22.26	32.89				2.20	18.97		0.04
MS2	W	6.40	1.68		1.14	0.21	0.09	0.80	6.83	82.85		
	Sp	9.12	20.88		0.53		0.18	39.12	3.95	26.21		
	Sp′	9.22	22.48		0.77	0.33	0.10	38.50	3.91	24.68		
	G	2.08	13.70	31.08	35.03	0.43		0.04	2.85	14.66		0.14

B: brownmillerite; CA: calcium aluminate; G: gehlenite; L: larnite; Sp: Mg-Cr-spinel; W: wustite

Table 3
Standard elution test results for as-received and modified slag.

Standard leaching test (EN 12457-2) on 4 mm slag: 24 h deionized water 10 l/kg						
Element	Units	S1	MS1	S2	MS2	Limits
Ba	mg/l	0.80	0.68	4.97	0.14	1
V	μg/l	136	48	<5	33	250
Cr	μg/l	<5	<5	<5	<5	50
pH		11.9	10.7	11.4	10.6	5.5–12
Conductibility	μS/cm	487	315	1.800	206	

ICP-OES detection limit for Cr and V = 5 μg/l.

confirm the complete stability of the modified slag, further investigation was performed on the slag powder by varying the water/slag ratio.

4.1. Leaching tests with different liquid-to-solid ratios

The liquid-to-solid ratio is one of the fundamental factors in the interaction between slag and the environment. The concentration of elute substances depends on the solution's pH, the solubility of the substances and the kinetics of dissolution. An increase in the L/S ratio should help maintain the pH far from basic values while contemporaneously working in conditions far from the saturation limit [45].

The analyses were not only focused on dangerous heavy metals, but also on the main elements constituting the different phases (Al, Ca, Mg, Si) in order to correlate them with the leaching behavior of the slag. Fig. 4 reports the leaching tests results in term of dissolved amount of slag after the test (defined as weight loss, Fig. 4a) and water pH at the end of the leaching test (Fig. 4b) for the different L/S ratios. The effects of the liquid/solid ratio were quite evident for all of the samples: increasing the water volume caused a corresponding increase in the amount of dissolved slag. However, the effect on the modified slag was slightly less than that seen on the as-received samples. In fact, the modified slag weight loss was an order of magnitude lower than the as-received samples. Moreover, increasing the L/S ratio, the water pH also decreased. With the

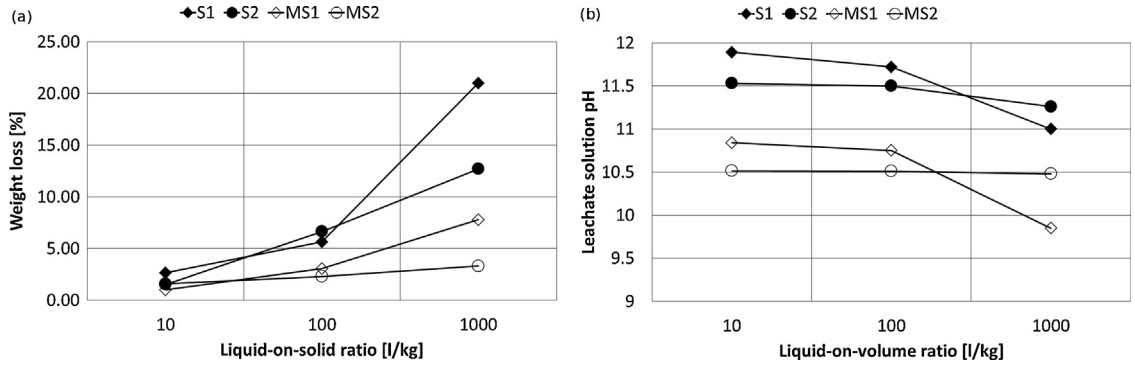

Fig. 4. Elution test result on powdered slag (a) weight loss and (b) water pH as a function of the L/S ratio.

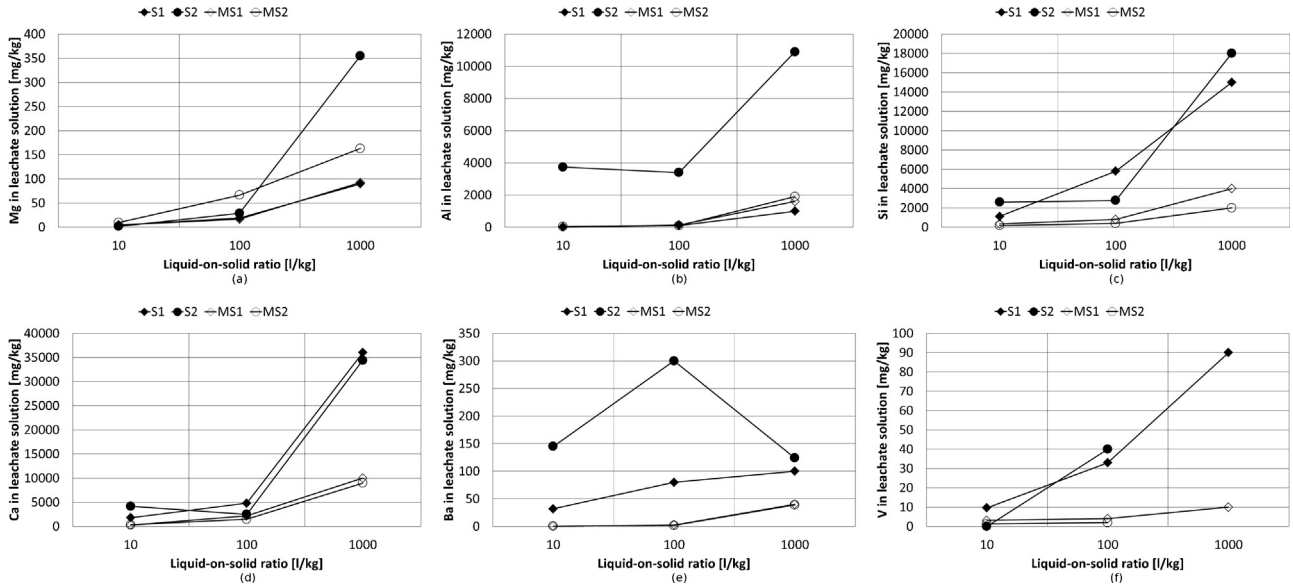

Fig. 5. Elution test results on powdered slag as a function of the water/slag ratio: (a) magnesium, (b) aluminum, (c) silicon, (d) calcium, (e) barium and (f) vanadium concentration in water.

water being less caustic at a high liquid-to-solid ratio, compared to the standard condition, the release of dangerous chemical species could potentially be enhanced (i.e. Ba) if the slag were not properly treated.

Fig. 5 summarizes the obtained results expressed in mg/kg in order to compare the different L/S ratios. The leaching test results obtained on the slag powders were compliant with the standard test result. Even if the concentration in elute water was higher for the powdered slag than the granulated one, the same leaching behavior was revealed. Samples belonging to batch #2 did not show vanadium release (Fig. 5f), as shown previously. In fact, the observed concentrations were close to the detectable limits in ICP-OES. The same conclusions should be stressed for chromium release. As for the standard test, including the powder test, Cr did not pose a problem for these slag.

Compared to treated samples, as-received samples showed higher concentrations for all of the investigated elements. Some differences between S1 and S2 slag were identifiable in regard to the Mg, Al and Ca leaching (Fig. 5a, b and d). Specifically, in Fig. 5a, the curve of S1 and MS1 samples are overlapped. Slag S2 had a higher concentration of those particular elements in the leachate than the S1 slag. In particular, Ca and Al release could be associated with brownmillerite dissolution since the S1 sample's composition did not contain this phase. The high Mg concentration in water seems associated to brownmillerite dissolution, too. Since brownmillerite forms close to wustite (Fig. 3c), brownmillerite dissolution could lead to Mg removal from wustite/brownmillerite interfaces, due to erosion phenomena. In the silica treated slag, the calcium was completely bound in gehlenite and its low concentration in the eluate acted as an index of the poor hydraulicity of gehlenite [46]. In the modified slag, aluminum was found in both Mg-Cr-spinel and in the gehlenite. The low concentration of Al in the water was synonymous with high spinel stability (and this behavior was confirmed by an undetectable concentration of Cr in the water). The tendency to retain Ba was confirmed in the treated slag: in the eluted solution the Ba concentration was one third that of the as-received samples (Fig. 5e).

The hypothesis, stressed on the basis of the elution tests results, was confirmed by an XRD analysis performed on leached powdered slag (Fig. 6). In order to compare the different spectra, normalization on a more intense wustite peak was performed. Wustite was selected because it should not react with water; in other words its dissolution rate is so low that it can be considered insoluble [47]. In as-received samples (in particular S2), the intensity of the larnite and brownmillerite peaks decreased as the L/S ratio increased (Fig. 6a). Spinel peaks also underwent intensity reduction. The different XRD spectrum showed that, by using a standard L/S ratio (10 l/kg), the interaction between slag and water was only cortical and pertained to only a limited portion of the material.

Effectively, during the standard leaching test, the water was quickly saturated by dissolved di-calcium silicate (and other hydraulic substances). Increasing the L/S ratio permitted work far from the larnite dissolution curve, allowing for the exacerbation of the slag and water contact conditions in order to clearly identify which phases were involved in the dissolution process. Fig. 7 shows the comparison between the di-calcium silicate dissolution curve and Si and Ca concentration in the leachate solution for the different slag investigated in this work. Slag tested at 10 l/kg had a concentration of Si and Ca close to the larnite dissolution curve. For this reason, no difference in XRD spectrum was noted before and after the leaching test. Then again, working with a high L/S ratio made it possible to maintain a leaching solution capable of dissolving a higher quantity of slag mass than at 10 l/kg. In fact, as reported by Nicoleau et al. [45], larnite undergoes a dissolution of approximately 60% after 30 min in water at 10,000 l/kg and

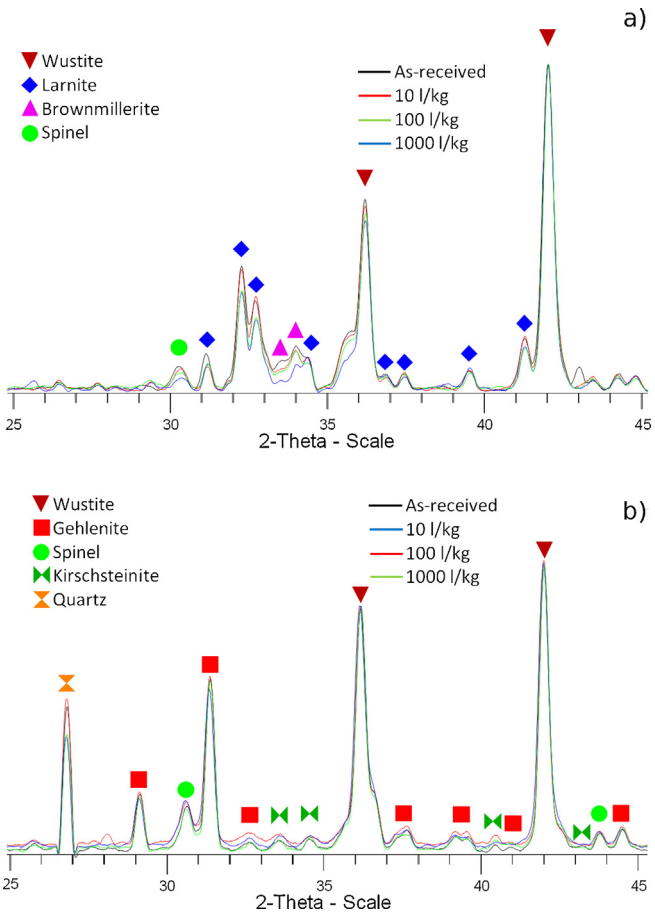

Fig. 6. XRD patterns of (a) S2 and (b) MS2 leached slag at different L/S ratios.

the dissolved fraction reaches almost the 100% with a L/S equal to 50,000 l/kg.

This conjecture was confirmed by SEM observation on the crushed slag surface (Fig. 8). By increasing the L/S ratio, the fraction of larnite dissolved increased rapidly whereas brownmillerite dissolution was clearly evident only at high water ratios (white arrows and circle in Fig. 8a–c). On the modified slag, diffraction patterns demonstrated the stability of the slag. Although the solid-to-liquid ratio increased, no modification in peaks intensity was evident.

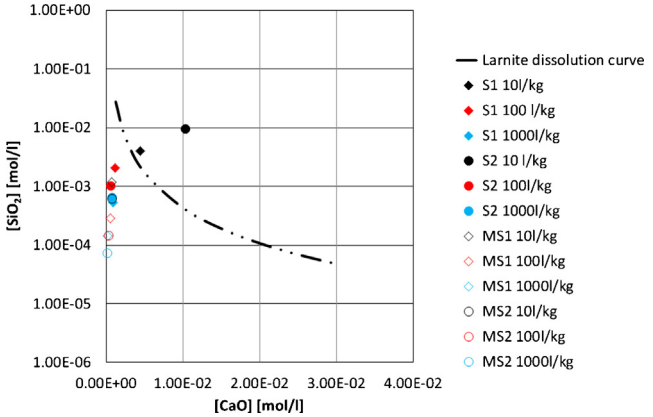

Fig. 7. Comparison between the larnite dissolution curve (K_{sp} = 40.3 × 10^{-8} [45]) and the Si and Ca concentration in leachate solution for the investigated slag [29,48].

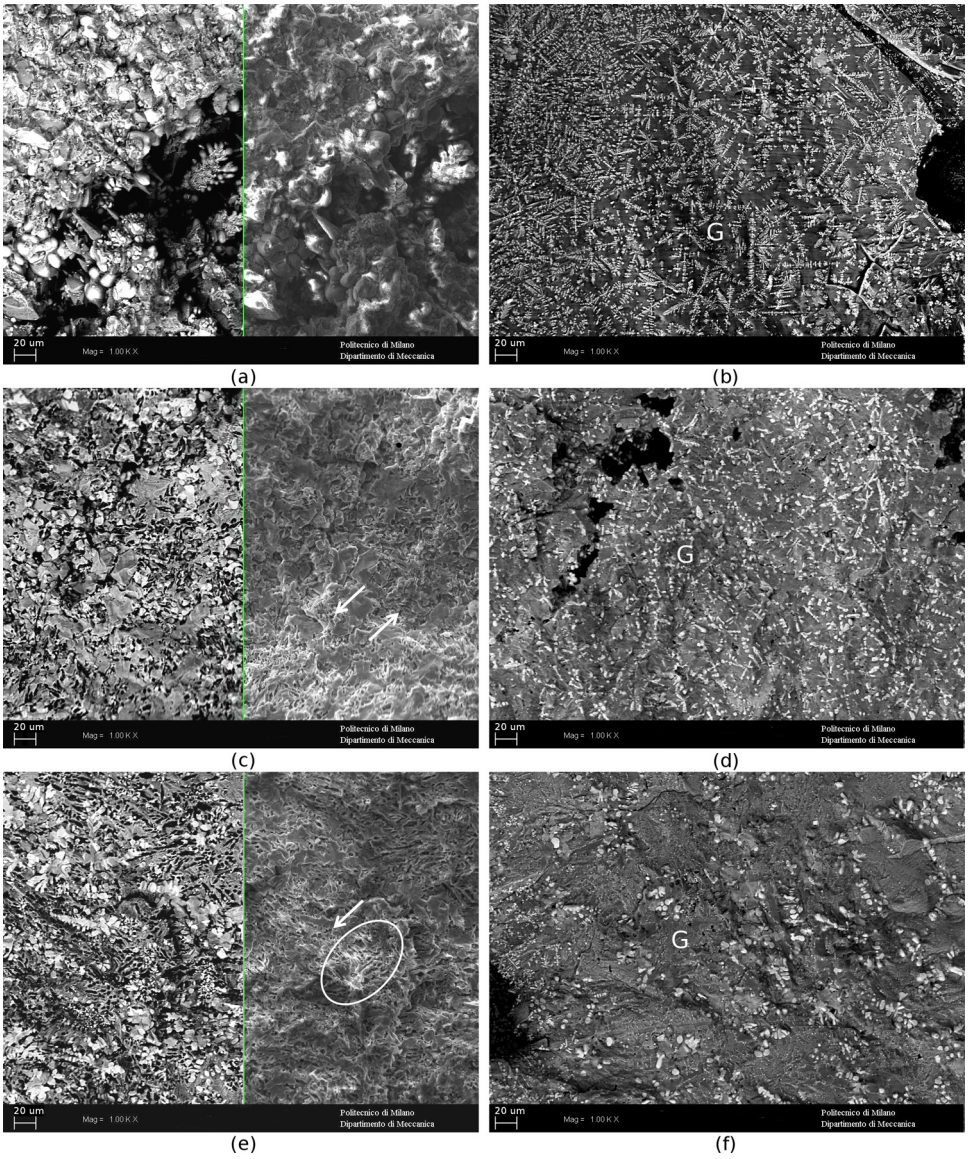

Fig. 8. SEM micrographies of leached slag at different L/S ratios: sample S1 at (a) 10, (c) 100, (e) 1000 l/kg and sample MS1 at (a) 10, (d) 100, (f) 1000 l/kg. White arrows and circle indicate the areas dissolved; G = gehlenite; white dendrites = wustite.

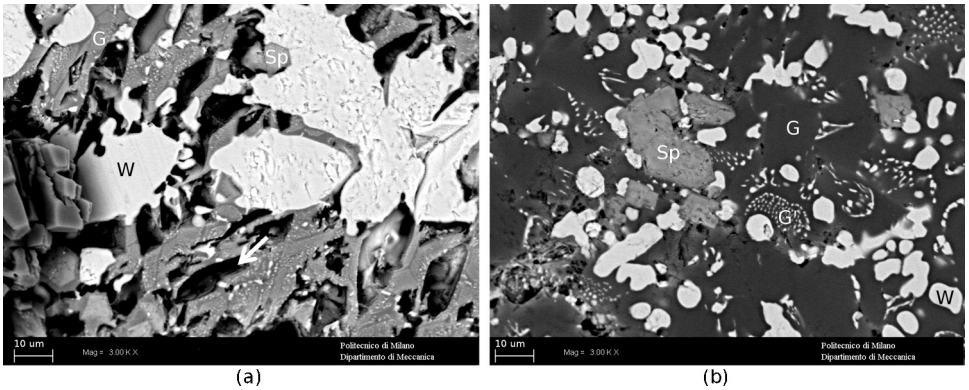

Fig. 9. SEM micrographies of leached slag (24 h) on polished section: (a) S1 and (b) MS1 samples. G = Gehlenite; Sp = Mg-Cr-spinel; W = wustite. White arrow indicates the dissolved larnite.

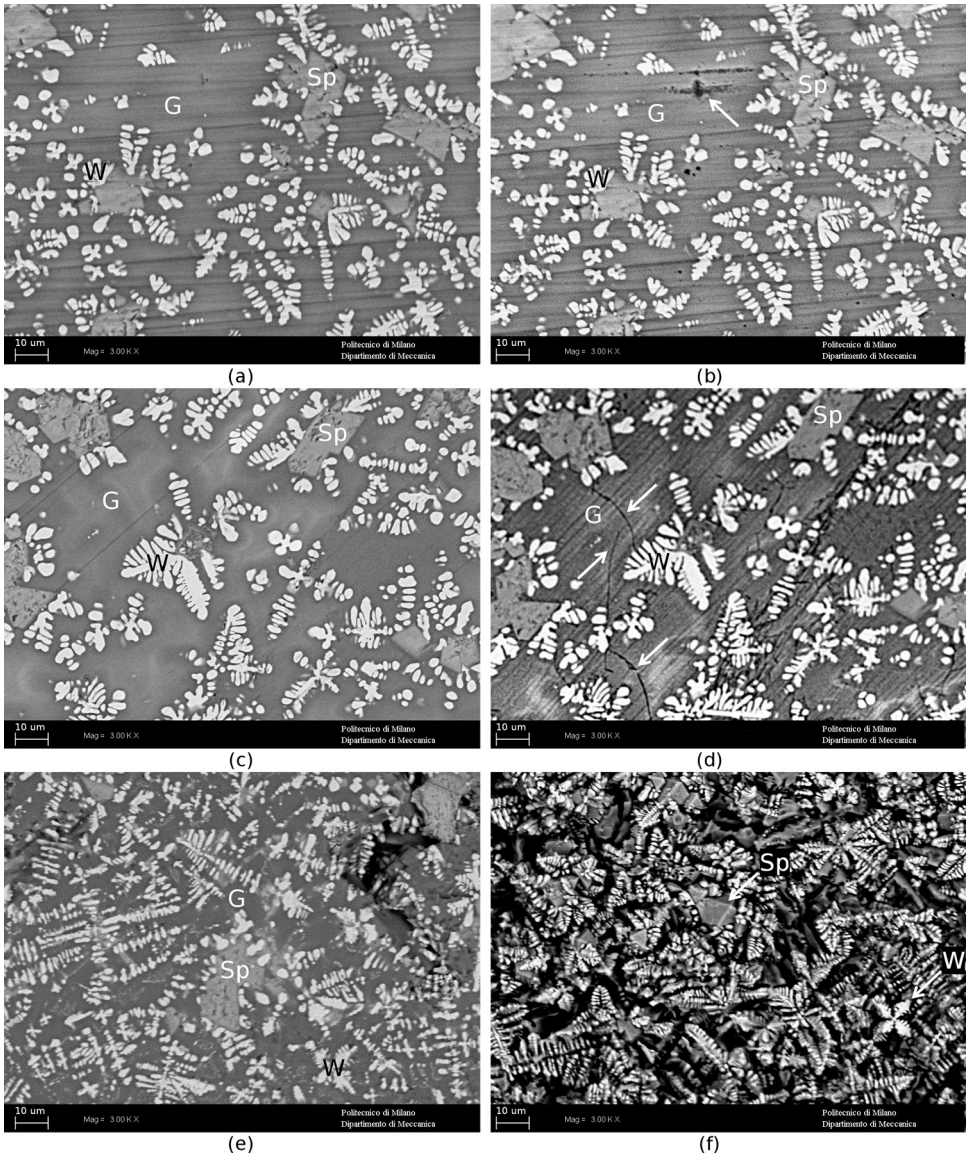

Fig. 10. SEM-BSE micrographies of leached slag on polished section. MS2 sample 30 days in water: (a) before, (b) after leaching test; MS2 sample 24 h in pH10 acqueous solution (c) before, (d) after leaching test; MS2 sample 24 h in pH 4 acquous solution (e) before,(f) after leaching test. G = gehlenite; Sp = Mg-Cr-spinel; W = wustite.

The SEM analyses were congruent with the diffraction analyses and confirmed the absolute integrity of the gehlenite matrix (Fig. 8d–f).

4.2. *Leaching test on a polished section*

In order to more precisely identify which phases were susceptible to water attack, a leaching test simulation was also performed on a polished section (Fig. 9a and b). This procedure was required because BSE probe contrast alone was insufficient to unambiguously identify the different phases on massive slag grains.

The polished slag was immersed in 350 ml of deionized water for 24 h and then observed by SEM in the same areas investigated during the morphological characterization (Fig. 2). In this case, the L/S ratio was extremely high (probably over 10,000 l/kg, since almost all the larnite features the slag was dissolved [45]) likely helping to maintain the water under saturated, with respect to the hydraulic phases, and thus avoiding pH modification.

These analyses clearly indicated that larnite was the most soluble phase in the water. However, a high amount of water was required to completely dissolve it (Fig. 9a). Brownmillerite was only partially eroded by water even if it seemed dissolved enough to release amounts of chromium and barium that had contributed to an increase in the water's total leachate content.

On the other hand, modified slag remained completely unaltered despite the very high liquid ratio, demonstrating the reliability of the inertization process (Fig. 9b).

Further tests on the polished section were conducted to stress the modified slag in the worst possible environmental conditions. Treated slag durability was investigated by submerging the modified samples in 350 ml of deionized water for 1 month. This test was a good indicator of the stability and the inertness of the gehlenite matrix and provided a qualitative indication about long-term slag behavior. In addition, two other experiments were carried out on modified slag evaluating them at different water pH values, in order to estimate their resistance far from the neutral conditions present in fresh water.

After 30 days in the water (Fig. 10a and b), the slag surface did not appear altered except in certain points corresponding with voids or porosity or where the chemical composition differed (white arrow in Fig. 10b). The obtained result was a clear indication of the very low hydraulicity of gehlenite. Moreover, wustite and spinel were also unaltered.

Different test results were obtained at different pH levels. In a basic environment (Fig. 10c and d), the slag seemed to resist quite well, even if the surface appeared consumed and some cracks were detectable (white arrows in Fig. 10d). However, the slag consumption only applied to the surface layer and the dissolution of the gehlenite matrix was limited. EDS analysis supported this hypothesis: the chemical composition of the investigated area differed less than 5% in the Si and Ca concentration before and after the elution test. This behavior corresponded with other research studies showing a limited release of the major chemical species constituting the slag when in contact with a basic environment [49,50]. On the contrary, the elution test in a pH 4 aqueous solution (Fig. 10e and f) showed nearly total dissolution of the gehlenite matrix. Contrariwise, also in this situation, wustite and spinels remain unaltered. This behavior confirmed the insolubility of wustite, and thus, its complete abnormality in the leaching process of dangerous chemical species. In this specific case, chromium spinels also seemed unaffected by the acidic environment.

The quartz addition, which maintained the slag in liquid form for a longer period of time, most likely caused the formation of spinels with stoichiometric composition, thus limiting the dissolution phenomena. Although the silica addition acidified the slag, it substantially remained basic. For this reason, the gehlenite matrix was completely dissolved when it came in contact with the acidic water. As reported by Yokohama et al. [49] and by Takahashi et al. [50], the calcium, magnesium and aluminum dissolution rates were higher in an acidic environment. Since these three elements are the major constituents of gehlenite, its dissolution was expected. These qualitative tests, under extreme environmental conditions, helped identify the lower and upper limit of modified slag applicability. On the basis of these results, we can assume that the use of such modified slag in environmental conditions ranging from between pH 8 and 6 should be exempt from environmental pollution and human health risks. Moreover, the experimental trials further demonstrated the efficiency of the slag treatment. The slag's structure remained intact in extreme conditions without disaggregation and dusting.

5. Conclusions

In conclusion, the efficiency of the inertization treatment through the addition of quartz to EAF slag was experimentally demonstrated.

- XRD and SEM analyses provided identification for the untreated slag of the more reacting phases with water regulating the release of dangerous chemical species. Larnite is the most soluble phase followed by brownmillerite. The insolubility of wustite has been confirmed whereas gehlenite-type phases were proved to be completely insoluble in basic and neutral environments.
- Slag use without any stabilization treatment could have dangerous environmental consequences, even when leaching limits are observed. In fact, in a long term scenario, the pH alteration due to cyclical carbonation phenomena could enhance the leaching of dangerous heavy metals, due to larnite and brownmillerite dissolution.
- The reaction between added SiO_2 and other silicates characterizing the slag microstructures promotes the formation of a gehlenite-type phase.
- Gehlenite is completely stable and assures safe and inert behavior in modified slag. If the slag chemical composition (wt%) is MgO: 2–4%; Al_2O_3: 7–10%; SiO_2: 15–25%; CaO: 15–25%; FeO: 35–40% stable gehlenite will be obtained.
- Modified slag releasing stability was demonstrated through leaching tests with variable L/S ratios, environmental pH levels and water exposure times.
- The modified slag can be considered a safe by-product and no more as hazardous waste. They could be used for both unbound applications and as aggregates without harming humans or polluting the environment, reducing the total amount of this by-product disposed in landfill.

List of phases

Phase	Definition	Formula	Symbol
Akermanite	Calcium-magnesium silicate	$Ca_2MgSi_2O_7$ ($2CaO{\cdot}MgO{\cdot}2SiO_2$)	A
Anorthite	Calcium-aluminum silicate	$CaAl_2Si_2O_8{\cdot}(CaO{\cdot}Al_2O_3{\cdot}2SiO_2)$	An
Bredigite	α di-calcium silicate	$Ca_7Mg(SiO_4)_4{\cdot}(7CaO{\cdot}MgO{\cdot}4SiO_2)$	Br
Brownmillerite	Tetra-calcium aluminate ferrite	$Ca_2(Al,Fe)_2O_5{\cdot}(4CaO{\cdot}Al_2O_3{\cdot}Fe_2O_3)$	B
Gehlenite	Calcium-aluminum silicate	$Ca_2Al(AlSi)O_7{\cdot}(2CaO{\cdot}Al_2O_3{\cdot}SiO_2)$	G
Kirschsteinite	Calcium olivine	$CaFeSiO_4{\cdot}(CaO{\cdot}FeO{\cdot}SiO_2)$	K
Larnite	β or γ di-calcium silicate	$Ca_2SiO_4{\cdot}(2CaO{\cdot}SiO_2)$	L
Mayenite	Calcium aluminate	$Ca_{12}Al_{14}O_{33}{\cdot}(12CaO{\cdot}7Al_2O_3)$	CA
Mg-Cr-spinel	Magnesiochromite (spinel)	$MgCr_2O_4/(Mg,Fe)(Al,Cr)_2O_4$	Sp
Wustite	Iron oxide	(Fe, Mg, Mn)O/MgO-FeO	W

Acknowledgments

The authors would like to acknowledge Simone and Umberto Di Landro (DILAB labs, Crema (CR), Italy) and Thierry Vincent (École des mines d'Alès, C2MA, Alès, France) for the ICP-OES analyses.

References

[1] S. Sorlini, A. Sanzeni, L. Rondi, Reuse of steel slag in bituminous paving mixtures, J. Hazard. Mater. 209–210 (2012) 84–91.
[2] T. Sofilic, V. Merle, A. Rastovcan-Mioc, M. Cosic, U. Sofilic, Steel slag instead natural aggregates in asphalt mixture, Arch. Metall. Mater. 55-3 (2010) 657–668.
[3] J. Alexandre, J.Y. Boudonnet, Les laitiers d'aciérie LD et leurs utilisations routières, Laitiers sidérurgiques 75 (1993) 57–62.
[4] B.B. Lind, A.M. Faellman, L.B. Larsson, Environmental impact of ferrochrome slag in road construction, Waste Manage. 21 (2001) 255–264.
[5] A.R. Dawson, R.C. Elliot, G.M. Rowe, J. Williams, An assessment of the suitability of some industrial by-products for use in pavement bases in the United Kingdom, Transp. Res. Rec. 1486 (1995) 114–123.
[6] S. Wu, Y. Xue, Q. Ye, Y. Chen, Utilization of steel slag as aggregates for stone mastic asphalt (SMA) mixtures, Build Environ. 42 (2007) 2580–2585.
[7] Internet reference http://www.euroslag.com/products/statistics/Statistic_2010_download.pdf
[8] G.-H. Zeng, J.A. Kozinski, Solid Waste Remediation in the Metallurgical Industry: Application and Environmental Impact, McGill Metals Processing Center, Department of Mining and Metallurgical Engineering, McGill University, 1996.
[9] H. Moltz, J. Geiseler, Products of steel slags an opportunity to save natural resources, Waste Manage. 21 (2001) 258–293.
[10] P. Chaurand, J. Rose, V. Briois, L. Olivi, J.-L. Hazemann, J. Domas, J.-Y. Bottero, O. Proux, Environmental impacts of steel slag reused in road construction:

a crystallographic and molecular (XANES) approach, J. Hazard. Mater. B139 (2007) 537–542.
[11] M. Del Fabbro, M. Stefanutti, C. Ceschia, Impiego di derivati delle scorie di forno ad arco elettrico come Materiale eco-compatibile nella sovrastruttura stradale, in: Proceedings of XI S.I.I.V Conference, Verona (Italy), 2001.
[12] A. Yılmaz, Use of Ferrochromium and Silico-ferro-chromium Slag and Silica Fume in road construction, PhD Thesis, Department of Civil Engineering, University of Suleyman Demirel, Isparta, 2008.
[13] S. Igarashi, M. Kawamura, N. Arano, S. Kawaguchi, Mechanical properties of mortar containing high-carbon ferrochromium slag as an aggregate, in: Proceedings of the International Conference on Engineering Materials, Ottawa (Canada), 1997, pp. 67–71.
[14] A. Yılmaz, Investigation of electric-arc furnace slag and silica fume of antalya ferrochrome establishment, as filler material in asphalt concrete, MS Thesis, Akdeniz University, Antalya, 2002.
[15] J. Zelic, Properties of concrete pavements prepared with ferrochromium slag as concrete aggregate, Cement Concrete Res. 35 (2005) 2340–2349.
[16] L. Muhmood, S. Vitta, D. Venkateswaran, Cementitious and pozzolanic behavior of electric arc furnace steel slags, Cement Concrete Res. 39 (2009) 102–109.
[17] V. Ducman, A. Mladenovič, The potential use of steel slag in refractory concrete, Mater. Charact. 62 (2011) 716–723.
[18] A. Van Zomeren, S.R. van der Laan, H.B.A. Kobesen, W.J.J. Huijgen, R.N.J. Comans, Changes in mineralogical and leaching properties of converter steel slag resulting from accelerated carbonation at low CO_2 pressure, Waste Manage. 31 (2011) 2236–2244.
[19] C.J. Engelsen, H.A. van der Sloot, G. Wibetoe, H. Justnes, W. Lund, E. Stoltenberg-Hansson, Leaching characterisation and geochemical modelling of minor and trace elements released from recycled concrete aggregates, Cement Concrete Res. 40 (2010) 1639–1649.
[20] C.J. Engelsen, G. Wibetoe, H.A. van der Sloot, W. Lund, G. Petkovic, Field site leaching from recycled concrete aggregates applied as sub-base material in road construction, Sci. Total Environ. 427–428 (2012) 86–97.
[21] S. Barella, A. Gruttadauria, F. Magni, C. Mapelli, D. Mombelli, Survey about safe and reliable use of EAF slag, ISIJ Int. 52-12 (2012) 2295–2302.
[22] D. Mombelli, C. Mapelli, A. Gruttadauria, C. Baldizzone, F. Magni, P.L. Levrangi, P. Simone, Analysis of electric arc furnace slag, Steel Res. Int. 83-11 (2012) 1012–1019.
[23] M. Gelfi, G. Cornacchia, R. Roberti, Investigations on leaching behavior of EAF steel slags, in: Proceeding of 6th European Slag Conference (EUROSLAG 2010), Madrid (Spain), 2010, pp. 57–169.
[24] L. De Windt, P. Chaurand, J. Rose, Kinetics of steel slag leaching: batch tests and modeling, Waste Manage. 31 (2011) 225–235.
[25] A.M. Faellman, Leaching of chromium and barium from steel slag in laboratory and field tests—a solubility controlled process? Waste Manage. 20 (2000) 149–154.
[26] C.J. Shi, J.S. Qian, High performance cementing materials from industrial slags—a review, Resour. Conserv. Recycl. 29-3 (29) (2000) 195–200.
[27] Forschungszentrum Karlsruhe Umweltforschungszentrum, Contaminated Soil, vol. 2, Proceedings of Seventh International FZK/TNO Conference on Contaminated Soil, Leipzig, Germany, 2000.
[28] Indipendet Evironmental Technical Evaluation Group (IETEG), Chromium (VI) Handbook, CRC Press, Baton Rouge, LA, 2004.
[29] H.F.W. Taylor, Cement Chemistry, Academic Press, London, UK, 1990, pp. 38–39.
[30] S. Brantley, J. Kubicki, A. White, Kinetics of Water–Rock Interaction, Springer, University Park (PA), 2007, pp. 161–165.
[31] S. Chandra, Waste Materials Used in Concrete Manufacturing, Noyes Publication, Eastwood (NJ), 1997, pp. 235–250.
[32] P. Drissen, A. Ehrenberg, M. Kühn, D. Mudersbach, Recent development in slag treatment and dust recycling, Steel Res. Int. 80-10 (2009) 737–745.
[33] H. Epstain, R.I. Iacobescu, Y. Pontikes, A. Malfliet, L. Machiels, P.T. Jones, B. Blanpain, Stabilization of $CaO–SiO_2–MgO$ (CSM) slags by recycled alumina, in: Proceeding of 7th European Slag Conference (EUROSLAG 2013), Ijmuiden (The Netherlands), 2013, pp. 108–117.
[34] Y.J. Kim, I. Nettleship, W.M. Kriven, Phase transformations in dicalcium silicate: II, TEM studies of crystallography, microstructure, and mechanism, J. Am. Ceram. Soc. 75-9 (1992) 2407–2419.
[35] T.E. Bridge, Bredigite, larnite and γ dicalcium silicates from marble canyon, Am. Miner. 51 (1996) 1766–1774.
[36] A.R. West, Solid State Chemistry and its Application, John Wiley & Sons Ltd., Hoboken, NJ, 1990.
[37] P.W. Scott, S.R. Critchley, F.C.F. Wilkinson, The chemistry and mineralogy of some granulated and pelletized blast furnace slags, Miner. Mag. 50 (1986) 141–147.
[38] M. Julli, Ecotoxicity and chemistry of leachates from blast furnace and basic oxygen steel slags, Australas. J. Ecotoxicol. 5 (1999) 123–132.
[39] D.M. Proctor, K.A. Fehling, E.C. Shay, J.L. Wittenborn, J.J. Green, C. Avent, R.D. Bigham, M. Connolly, B. Lee, T.O. Shepker, M.A. Zack, Physical and chemical characteristics of blast furnace, basic oxygen furnace, and electric arc furnace steel industry slags, Environ. Sci. Technol. 34 (2000) 1576–1582.
[40] J.A. Duffy, M.D. Ingram, I.D. Sommerville, Acid–base properties of molten oxides and metallurgical slags, J. Chem. Soc. Farad. T. 1: Phys. Chem. Condens. Phases 74 (1978) 1410–1419.
[41] H.A. van der Sloot, J.J. Dijkstra, Development of horizontally standardized leaching tests for construction materials: a material based or release based approach? in: Identical Leaching Mechanisms for Different Materials, ECN-C–04-060, Energy Research Centre of the Netherlands (ECN), 2004.
[42] E.M. Levin, C.E. Robbins, H.F. McMurdie, Phase Diagrams for Ceramist, vol. 1, The American Ceramic Society, Columbus (OH), 1964.
[43] W.A. Klemn, J. Skalny, Selective dissolution of clinker minerals and its applications Martin Marietta Technical Rep. 77 (1977) 26.
[44] J. Pera, A. Amrouz, Development of highly reactive metakaoline from paper sludge, Adv. Cement Based Mater. 7 (1998) 49–56.
[45] L. Nicoleau, A. Nonat, D. Perrey, The di- and tricalcium silicate dissolutions, Cement Concrete Res. 47 (2013) 14–30.
[46] H. Pöllmann, Mineralogy and crystal chemistry of calcium aluminate cement, in: Proceedings of the International Conference on Calcium Aluminate Cement, Edinburgh (Scotland), IOM Communications Ltd., London, 2001, pp. 14–30.
[47] E. Belhadj, C. Diliberto, A. Lecomte, Characterization and activation of basic oxygen furnace slag, Cement Concrete Comp. 34 (2012) 34–40.
[48] K.L. Scrivener, A. Nonat, Hydration of cementitious materials, present and future, Cement Concrete Res. 41 (2011) 651–665.
[49] S. Yokoyama, A. Suzuki, M. Izaki, M. Umemoto, Elution behavior of electronic arc furnace oxidizing slag into fresh water, Tetsu-to-Hagané 95-5 (2009) 434–443.
[50] Y. Takahashi, Y. Ogura, A. Ogawa, H. Kanematsu, S. Yokohama, An effective and economic strategy to restore acidified fresh water ecosystems with steel industrial byproducts, J. Water Environ. Technol. 10-4 (2012) 347–362.